Organic LETTERS

Letter

pubs.acs.org/OrgLett

Photoresponsive Toroidal Nanostructure Formed by Self-Assembly of Azobenzene-Functionalized Tris(phenylisoxazolyl)benzene

Hiroaki Adachi,[†] Yuko Hirai,[†] Toshiaki Ikeda,[†] Makoto Maeda,[‡] Ryo Hori,[§] Shoichi Kutsumizu,[§] and Takeharu Haino*[,†]

[†]Department of Chemistry, Graduate School of Science, Hiroshima University, 1-3-1 Kagamiyama, Higashi-Hiroshima 739-8526, Japan

[‡]Natural Science Center for Basic Research and Development, Hiroshima University, 1-3-1 Kagamiyama, Higashi-Hiroshima 739-8530, Japan

[§]Department of Chemistry and Biomolecular Science, Faculty of Engineering, Gifu University, Yanagido, Gifu 501-1193, Japan

Supporting Information

ABSTRACT: The self-assembly of tris(phenylisoxazolyl)benzene **1b** with photochemically addressable azobenzene moieties produced toroidal nanostructures, the formation and dissociation of which were reversibly regulated upon photoirradiation. **1b** displayed a mesogenic behavior. In the solution, the stacked assemblies along with their C_3 axes were formed. In the mesophase, two molecules of **1b** most likely adopted the antiparallel arrangement to stabilize the columnar organization. This assembling behavior most likely triggered the development of the supramolecular toroidal nanostructures.

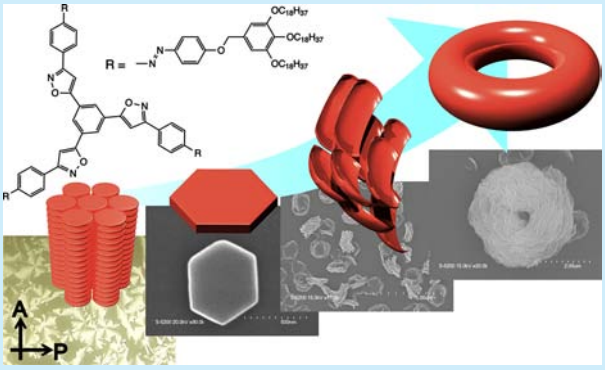

Spontaneous self-assembly of inorganic and organic molecules and polymers generates various nanostructures such as toroids, tubes, helices, disks, and fibers.[1,2] Among them, toroidal structures have unique annular shapes with various applications in nanoscale materials and devices.[3] Much effort has been directed toward the control of molecular organization in such unique toroidal nanostructures because their size, shape, and dimension determine the resulting properties and functions.[4] Although toroidal nanostructures have been produced in the self-assembly of polymers and molecules,[3c,5,6] a limited number of photoresponsive toroidal nanostructures have been developed.[7] Therefore, the development of toroidal nanostructures that can be controlled by photostimuli is a prime challenge for further exploring their applications.

The supramolecular organization of nanostructures relies on specific noncovalent interactions, which are notably sensitive to their molecular structures. The structural change of molecular components, which is induced by photostimuli, can vary the intermolecular interactions in the assembled state, which is fulfilled by introducing the photochromic functionalities. A photochromic π-conjugated molecular component can control the nano-organization processes using photostimuli. An azobenzene group as a photochemically addressable functionality is notably useful for developing photoresponsive supramolecular nanostructures.[8] We have reported that azobenzene-functionalized tris(phenylisoxazolyl)benzenes assembled to form fibrillar gel networks in organic solvents,[9] and the formation of organogels was reversibly regulated using photostimuli.[10] In the studies, intriguing nanostructures such as helices, tapes, and fibers were found as results of the assemblies. Herein, we report a photoresponsive toroidal nanostructure formed by the self-assembly of azobenzene-functionalized tris(phenylisoxazolyl)-benzene **1b** (Figure 1) and its mesogenic properties.

Tris(phenylisoxazolyl)benzenes **1a**−**c** gelled benzaldehyde, dioxane, benzyl chloride, diphenyl ether, anisole, and bonzonitrile (Figure S1); however, the critical gelation concentrations (CGC) were 25−200 g L^{-1} (Table S1). The gelators **1a**−**c** had modest CGC values compared to the previously reported tris(phenyl-

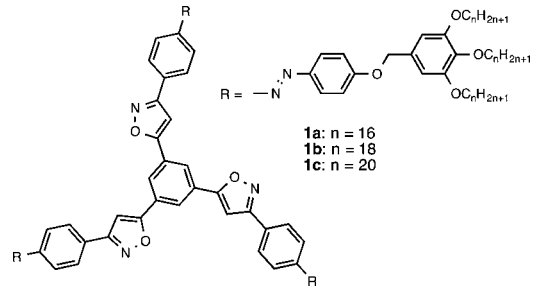

Figure 1. Azobenzene-functionalized gelators **1a**−**c**.

Received: December 21, 2015
Published: February 24, 2016

DOI: 10.1021/acs.orglett.5b03622
Org. Lett. 2016, 18, 924−927

isoxazolyl)benzene-based gelators. Scanning electron microscopy (SEM) of cast films, which were prepared from solutions of **1a–c** in benzene, gave us insights into gelation. Surprisingly, toroidal nanostructures of **1b** were found when **1a** and **1c** contrastively produced sheet-like morphologies, which implies that the size of the alkyl side chains affects the nanostructure formation (Figure 2a–c). The toroids had a notably uniform

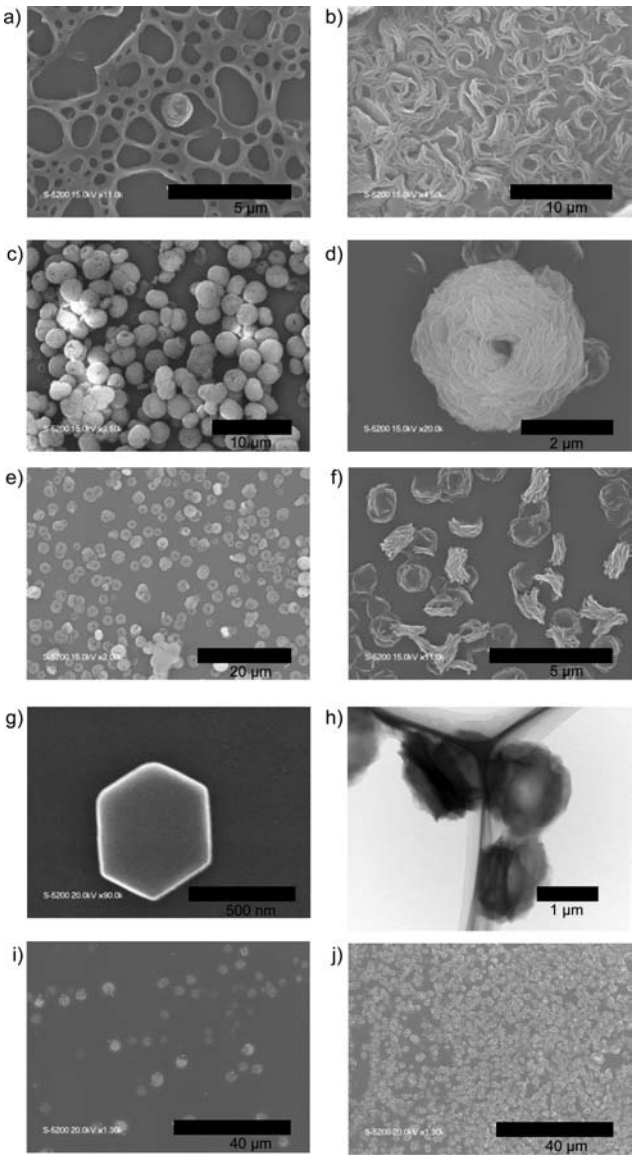

Figure 2. SEM images of cast films that were prepared from benzene solutions of (a) **1a** (0.5 mmol L^{-1}), (b) **1c** (0.5 mmol L^{-1}), and (c) 1.0 mmol L^{-1}; (d) expanded image of (c); (e) 0.5 mmol L^{-1}; (f) 0.1 mmol L^{-1}; and (g) 0.01 mmol L^{-1} of **1b**. (h) Transmission electron microscopy (TEM) image of **1b**. (i) SEM image of the cast film that was prepared from a solution of (c) after irradiation at 365 nm for 30 min and (j) SEM image of the cast film that was prepared from a solution of (i) and left standing at room temperature for a few hours.

diameter of 3.20 ± 0.09 μm and a height of 2.3 ± 0.1 μm (Figure 2c,d), and pierced holes with a diameter of 490 ± 40 nm were confirmed using a transmission electron microscopy (TEM) image (Figure 2h). The size of the toroids depended on the concentration of the **1b** solution; the 0.5 mmol L^{-1} solution produced smaller toroids with a diameter of 2.7 ± 0.2 μm and a height of 2.1 ± 0.1 μm (Figure 2e). Further dilution destroyed the toroidal nanostructures, and the stacked sheets were found (Figure 2f). Eventually, a distorted hexagonal sheet (500 ± 100 nm) was obtained from a solution concentration of 0.01 mmol L^{-1} (Figure 2g).

It is known that the *cis*-isomerization of the azobenzene moieties strongly interferes with the molecular assembly. This knowledge encouraged us to examine the photoinduced regulation of the nanostructure formation. After a 1.0 mmol L^{-1} solution of **1b** in benzene was irradiated at 365 nm for 30 min, a cast film deposited on a glass plate was subjected to SEM observation. The toroidal nanostructures completely collapsed to produce agglomerates (Figure 2i). The *cis*-form of the azobenzene moieties was transferred to the *trans*-form when the solution was left standing at rt for a few hours. The toroidal nanostructures were eventually restored in the cast film on a glass plate (Figure 2j).

To gain detailed insight into the nanostructure formation, the self-assembling behavior in solution was studied. The ^{1}H NMR signals of compound **1b** were concentration-dependent in chloroform-d_1 (Figure 3). The aromatic signals moved upfield

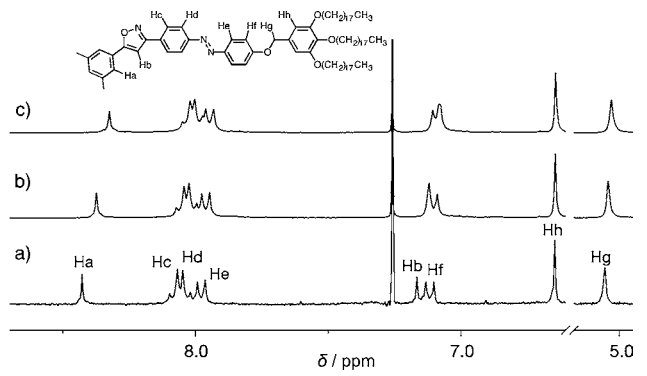

Figure 3. ^{1}H NMR spectra of **1b** at 23 °C in chloroform-d_1. The concentrations: (a) 2.3, (b) 9.2, (c) 40.6 mmol L^{-1}.

with the increase in solution concentration. The plot of the chemical shift changes of the protons versus the concentration of **1b** shows hyperboric curves. By applying the isodesmic model (Figure S4),[11] the nonlinear curve-fitting analysis of the curves resulted in the estimate complexation-induced shifts (Ha: −1.57, Hb: −1.25, Hc: −0.74, Hd: −0.67, He: −0.49, Hf: −0.42, Hg: −0.42, Hh: −0.09 ppm) with an association constant of 7.3(5) L mol^{-1} (Table S2).[12] The complexation-induced shifts decreased with increasing distance of the protons from the C_3 axis of **1b**, which indicates that flat aromatic compound **1b** stacks in a columnar fashion along the C_3 axis.

The self-assembly of **1b** was facilitated in benzene. Dynamic light scattering measurements of a solution of **1b** showed that large aggregates with hydrodynamic diameters of 260 ± 100 nm were formed (Figure 4). Upon irradiation at 365 nm, the autocorrelation function of the scattering intensity fluctuations decayed within less than 1 μs, which indicates that most large aggregates disappeared because of the *trans-to-cis* isomerization of the azobenzene moieties (Figure S7). The reirradiation of the solution at 450 nm resulted in the light-induced reverse isomerization of the azobenzene moieties, which restored the large aggregates with diameters of 290 ± 130 nm.[13] Accordingly, **1b** demonstrated the perfect reversibility of the formation–dissociation of the supramolecular aggregates, which was directed by the light-driven isomerization of the azobenzene moieties.

DOI: 10.1021/acs.orglett.5b03622
Org. Lett. 2016, 18, 924–927

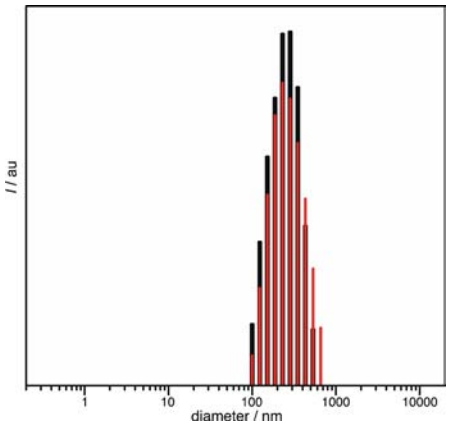

Figure 4. Dynamic light scattering of a benzene solution of **1b** (0.2 mmol L^{-1}): (black) before the isomerization and (red) after irradiation at 450 nm to the solution of *cis*-isomerized **1b**.

Compound **1b** exhibited mesogenic behavior, which provided insight into the initial stage of the nanostructure formation. The phase transition was studied using POM and DSC. In the DSC measurement from 30 to 175 °C, three distinct endothermic peaks were observed at 46.3, 136.5, and 166.9 °C (Figure 5a). The

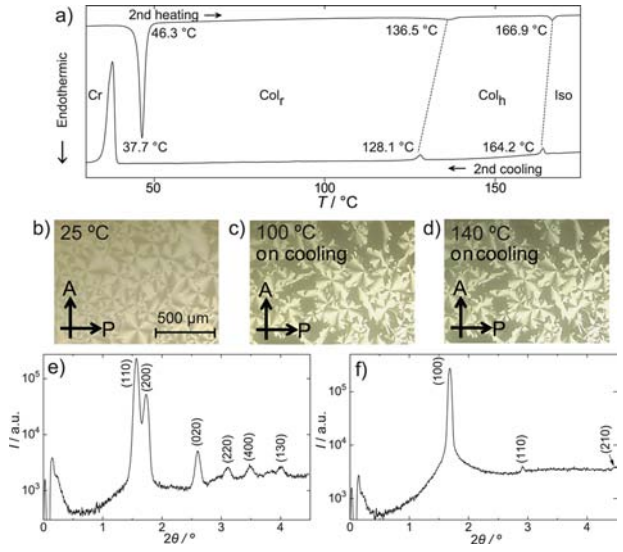

Figure 5. (a) DSC curves of **1b** in the second heating and cooling processes and POM images obtained on cooling. POM images at (b) 25, (c) 100, and (d) 140 °C. SAXS patterns at (e) 73.4 and (f) 146.1 °C on cooling. Values in parentheses are Miller indices.

transition recorded using DSC at 166.9 °C corresponded to the clearing point to isotropic liquid in the POM observation. Upon cooling **1b** from the isotropic liquid phase, two columnar liquid crystalline phases with pseudofocal conic textures were observed from the clearing point to the melting point (Figures 5c,d). The two columnar phases did not show any characteristic difference in texture. The molecular arrangements of **1b** in the columnar phases were disclosed using SAXS. The SAXS study at 73.4 °C developed six peaks (Figure 5e), which were consistent with a rectangular columnar (Col_r) lattice with the lattice parameters of a = 10.18 nm and b = 6.78 nm, whereas a hexagonal columnar (Col_h) lattice (a = 6.06 nm) was determined at 146.1 °C (Figure 5f). In the wide-angle region, two broad halos were observed corresponding to the distances of the disk-like units (c = 0.47 and 0.49 nm at 73.9 and 146.7 °C, respectively), which are most likely consistent with the mean distance of the liquid-like side chains that were segregated from the rigid aromatic core. Based on the assumption of a material density of $\delta \simeq 1$ g cm^{-3}, two molecules of **1b** roughly fill each columnar unit. An antiparallel organization of two **1b** molecules fairly fulfilled the experimental diameter of the hexagonal columnar unit (a = 6.06 nm), which suggests that flexible alkyl side chains are fully interdigitated and stabilize the columnar organization.

A plausible picture of the organization of the toroidal nanostructure is illustrated in Scheme 1. The organization is

Scheme 1. Plausible Mechanism of the Self-Assembling Process into the Toroidal Nanostructures

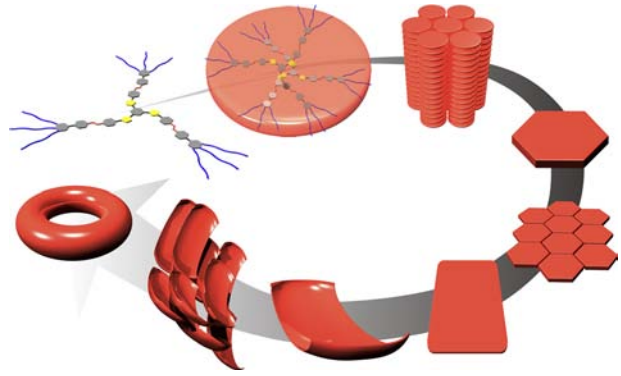

involved in multistep processes at the nanometer scale. The isoxazole moieties are responsible for the intermolecular dipole–dipole and $\pi-\pi$ stacking interactions that direct the supramolecular polymerization of **1b** in a columnar fashion in both solution and bulk. The long alkyl side chains are segregated at the periphery of the columnar assemblies. This crowded organization of the side chains can facilitate the attractive van der Waals interactions and result in the bundles of supramolecular polymeric assemblies. The hexagonal sheets that are slightly distorted are produced from further growth of the assemblies. The sheets stack in bent layers. The toroidal nanostructures are formed.

In summary, C_3-symmetric tris(phenylisoxazolyl)benzene **1b** with photochemically addressable azobenzene moieties assembled to form toroidal nanostructures. The organization of the toroidal nanostructures was reversibly controlled using photostimuli. The size and dimension of the toroidal nanostructures were concentration-dependent. The dilution of a **1b** solution destroyed the nanostructures and resulted in a hexagonal sheet. **1b** displayed mesogenic behavior. Rectangular and hexagonal columnar liquid crystalline phases were found. In the solution, stacked assemblies were formed along their C_3 axis. This assembling behavior most likely triggered the development of the supramolecular toroidal nanostructures. The interesting toroidal nanostructures have large cavities, where a guest molecule can be accommodated.[14] The photoresponsive feature of the toroidal nanostructure can offer the reversible uptake regulation and release a guest via photostimuli.

■ ASSOCIATED CONTENT

Supporting Information

The Supporting Information is available free of charge on the ACS Publications website at DOI: 10.1021/acs.orglett.5b03622.

DOI: 10.1021/acs.orglett.5b03622
Org. Lett. 2016, 18, 924–927

Experimental procedures and characterization data, gelation properties, and additional spectroscopic, X-ray scattering, calculation results, and ^{1}H and ^{13}C NMR spectra of new synthetic compounds (PDF)

AUTHOR INFORMATION

Corresponding Author

*E-mail: haino@hiroshima-u.ac.jp.

Notes

The authors declare no competing financial interest.

ACKNOWLEDGMENTS

This work was supported by Grant-in-Aids for Scientific Research (B), (C) (Nos. 15H00752, 15KT0145 for T.H. and No. 25410091 for S.K.), and for Young Scientists (B) (26810051 for T.I.) of JSPS and Grant-in-Aids for Scientific Research in Innovative Areas: "Stimuli-responsive Chemical Species for the Creation of Functional Molecules" and "New Polymeric Materials Based on Element-Blocks" (Nos. 15H00946, 15H00752) of MEXT (both for T.H.). The contributions from the Sekisui Chemical Grant Program for Research are greatly appreciated.

REFERENCES

(1) (a) Whitesides, G. M.; Grzybowski, B. *Science* **2002**, *295*, 2418−2421. (b) Jain, S.; Bates, F. S. *Science* **2003**, *300*, 460−464. (c) Shimizu, T.; Masuda, M.; Minamikawa, H. *Chem. Rev.* **2005**, *105*, 1401−1443. (d) Ajayaghosh, A.; Praveen, V. K. *Acc. Chem. Res.* **2007**, *40*, 644−656. (e) Palmer, L. C.; Stupp, S. I. *Acc. Chem. Res.* **2008**, *41*, 1674−1684. (f) Lim, Y. B.; Moon, K. S.; Lee, M. *Chem. Soc. Rev.* **2009**, *38*, 925−934. (g) Zhou, Y. F.; Yan, D. Y. *Chem. Commun.* **2009**, 1172−1188. (h) Wang, C.; Wang, Z. Q.; Zhang, X. *Acc. Chem. Res.* **2012**, *45*, 608−618. (i) Yagai, S. *Bull. Chem. Soc. Jpn.* **2015**, *88*, 28−58.

(2) (a) Ghadiri, M. R.; Granja, J. R.; Milligan, R. A.; Mcree, D. E.; Khazanovich, N. *Nature* **1993**, *366*, 324−327. (b) Kim, H. S.; Hartgerink, J. D.; Ghadiri, M. R. *J. Am. Chem. Soc.* **1998**, *120*, 4417−4424. (c) Engelkamp, H.; Middelbeek, S.; Nolte, R. J. M. *Science* **1999**, *284*, 785−788. (d) Zastavker, Y. V.; Asherie, N.; Lomakin, A.; Pande, J.; Donovan, J. M.; Schnur, J. M.; Benedek, G. B. *Proc. Natl. Acad. Sci. U. S. A.* **1999**, *96*, 7883−7887. (e) Hartgerink, J. D.; Beniash, E.; Stupp, S. I. *Science* **2001**, *294*, 1684−1688. (f) Valery, C.; Paternostre, M.; Robert, B.; Gulik-Krzywicki, T.; Narayanan, T.; Dedieu, J. C.; Keller, G.; Torres, M. L.; Cherif-Cheikh, R.; Calvo, P.; Artzner, F. *Proc. Natl. Acad. Sci. U. S. A.* **2003**, *100*, 10258−10262. (g) Percec, V.; Dulcey, A. E.; Balagurusamy, V. S. K.; Miura, Y.; Smidrkal, J.; Peterca, M.; Nummelin, S.; Edlund, U.; Hudson, S. D.; Heiney, P. A.; Hu, D. A.; Magonov, S. N.; Vinogradov, S. A. *Nature* **2004**, *430*, 764−768. (h) Yan, D. Y.; Zhou, Y. F.; Hou, J. *Science* **2004**, *303*, 65−67. (i) Elgersma, R. C.; Meijneke, T.; Posthuma, G.; Rijkers, D. T. S.; Liskamp, R. M. J. *Chem. - Eur. J.* **2006**, *12*, 3714−3725. (j) Zubarev, E. R.; Sone, E. D.; Stupp, S. I. *Chem. - Eur. J.* **2006**, *12*, 7313−7327. (k) Kim, J.-K.; Lee, E.; Kim, M.-C.; Sim, E.; Lee, M. *J. Am. Chem. Soc.* **2009**, *131*, 17768−17770. (l) Han, J.-H.; Lee, S.; Yoo, D.; Lee, J.-H.; Jeong, S.; Kim, J.-G.; Cheon, J. *J. Am. Chem. Soc.* **2013**, *135*, 3736−3739. (m) Song, B.; Liu, B.; Jin, Y.; He, X.; Tang, D.; Wu, G.; Yin, S. *Nanoscale* **2015**, *7*, 930−935.

(3) (a) Thordarson, P.; Bijsterveld, E. J. A.; Rowan, A. E.; Nolte, R. J. M. *Nature* **2003**, *424*, 915−918. (b) Mishra, A.; Ma, C. Q.; Bauerle, P. *Chem. Rev.* **2009**, *109*, 1141−1276. (c) Suresh, V. M.; George, S. J.; Maji, T. K. *Adv. Funct. Mater.* **2013**, *23*, 5585−5590.

(4) (a) Zhang, J.; Li, X.; Li, X. *Prog. Polym. Sci.* **2012**, *37*, 1130−1176. (b) Kim, Y.; Li, W.; Shin, S.; Lee, M. *Acc. Chem. Res.* **2013**, *46*, 2888−2897.

(5) (a) Conwell, C. C.; Vilfan, I. D.; Hud, N. V. *Proc. Natl. Acad. Sci. U. S. A.* **2003**, *100*, 9296−9301. (b) Pochan, D. J.; Chen, Z. Y.; Cui, H. G.; Hales, K.; Qi, K.; Wooley, K. L. *Science* **2004**, *306*, 94−97. (c) Carlson, J. C. T.; Jena, S. S.; Flenniken, M.; Chou, T. F.; Siegel, R. A.; Wagner, C. R. *J. Am. Chem. Soc.* **2006**, *128*, 7630−7638. (d) Nie, Z.; Fava, D.; Kumacheva, E.; Zou, S.; Walker, G. C.; Rubinstein, M. *Nat. Mater.* **2007**, *6*, 609−614. (e) Huang, H.; Chung, B.; Jung, J.; Park, H.-W.; Chang, T. *Angew. Chem., Int. Ed.* **2009**, *48*, 4594−4597. (f) Wang, B. G.; Shum, H. C.; Weitz, D. A. *ChemPhysChem* **2009**, *10*, 641−645. (g) Carroll, G. T.; Jongejan, M. G. M.; Pijper, D.; Feringa, B. L. *Chem. Sci.* **2010**, *1*, 469−472. (h) Lim, Y. B.; Lee, E.; Lee, M. *Macromol. Rapid Commun.* **2011**, *32*, 191−196. (i) Park, I.-S.; Yoon, Y.-R.; Jung, M.; Kim, K.; Park, S.; Shin, S.; Lim, Y.-B.; Lee, M. *Chem. - Asian J.* **2011**, *6*, 452−458. (j) Cardiel, J. J.; Tonggu, L.; Dohnalkova, A. C.; de la Iglesia, P.; Pozzo, D. C.; Wang, L. G.; Shen, A. Q. *ACS Nano* **2013**, *7*, 9704−9713. (k) Au-Yeung, H.-L.; Leung, Y.-L.; Tam, A. Y.-Y.; Yam, V. W.-W. *J. Am. Chem. Soc.* **2014**, *136*, 17910−17913. (l) Mazzier, D.; Mba, M.; Zerbetto, M.; Moretto, A. *Chem. Commun.* **2014**, *50*, 4571−4574. (m) Phillips, A. J.; Littlejohn, J.; Yewdall, N. A.; Zhu, T.; Valery, C.; Pearce, F. G.; Mitra, A. K.; Radjainia, M.; Gerrard, J. A. *Biomacromolecules* **2014**, *15*, 1871−1881.

(6) (a) Shoji, O.; Tanaka, H.; Kawai, T.; Kobuke, Y. *J. Am. Chem. Soc.* **2005**, *127*, 8598−8599. (b) Yagai, S.; Mahesh, S.; Kikkawa, Y.; Unoike, K.; Karatsu, T.; Kitamura, A.; Ajayaghosh, A. *Angew. Chem., Int. Ed.* **2008**, *47*, 4691−4694. (c) Gomez-Esteban, S.; Pezella, M.; Domingo, A.; Hennrich, G.; Gomez-Lor, B. *Chem. - Eur. J.* **2013**, *19*, 16080−16086. (d) Li, W.; Li, J.; Lee, M. *Chem. Commun.* **2013**, *49*, 8238−8240. (e) Wang, X.; Duan, P.; Liu, M. *Chem. - Eur. J.* **2013**, *19*, 16072−16079.

(7) (a) Yagai, S.; Yamauchi, M.; Kobayashi, A.; Karatsu, T.; Kitamura, A.; Ohba, T.; Kikkawa, Y. *J. Am. Chem. Soc.* **2012**, *134*, 18205−18208. (b) Kameta, N.; Masuda, M.; Shimizu, T. *Chem. - Eur. J.* **2015**, *21*, 8832−8839.

(8) (a) Shimizu, Y.; Kurobe, A.; Monobe, H.; Terasawa, N.; Kiyohara, K.; Uchida, K. *Chem. Commun.* **2003**, 1676−1677. (b) Yagai, S.; Nakajima, T.; Kishikawa, K.; Kohmoto, S.; Karatsu, T.; Kitamura, A. *J. Am. Chem. Soc.* **2005**, *127*, 11134−11139. (c) Kumar, N. S. S.; Varghese, S.; Narayan, G.; Das, S. *Angew. Chem., Int. Ed.* **2006**, *45*, 6317−6321. (d) Akazawa, M.; Uchida, K.; de Jong, J. J. D.; Areephong, J.; Stuart, M.; Caroli, G.; Browne, W. R.; Feringa, B. L. *Org. Biomol. Chem.* **2008**, *6*, 1544−1547.

(9) (a) Haino, T.; Tanaka, M.; Fukazawa, Y. *Chem. Commun.* **2008**, 468−470. (b) Haino, T.; Saito, H. *Synth. Met.* **2009**, *159*, 821−826. (c) Tanaka, M.; Ikeda, T.; Mack, J.; Kobayashi, N.; Haino, T. *J. Org. Chem.* **2011**, *76*, 5082−5091. (d) Ikeda, T.; Masuda, T.; Hirao, T.; Yuasa, J.; Tsumatori, H.; Kawai, T.; Haino, T. *Chem. Commun.* **2012**, *48*, 6025−6027. (e) Ikeda, T.; Masuda, T.; Takayama, M.; Adachi, H.; Haino, T. *Org. Biomol. Chem.* **2016**, *14*, 36. (f) Ikeda, T.; Takayama, M.; Kumar, J.; Kawai, T.; Haino, T. *Dalton Trans.* **2015**, *44*, 13156−13162. (g) Ikeda, T.; Masuda, T.; Takayama, M.; Adachi, H.; Haino, T. *Org. Biomol. Chem.* **2016**, *14*, 36−39.

(10) (a) Haino, T.; Saito, H. *Aust. J. Chem.* **2010**, *63*, 640−645. (b) Haino, T.; Hirai, Y.; Ikeda, T.; Saito, H. *Org. Biomol. Chem.* **2013**, *11*, 4164−4170.

(11) *Supramolecular Polymers*, 2nd ed.; Ciferri, A., Ed.; CRC Press - Taylor & Francis: Boca Raton, FL, 2005.

(12) Association constants in chloroform-d_1 are 6.3(8), 7.3(5), and 8.1(8) L mol^{-1} for **1a**, **1b**, and **1c**, respectively. The increase of the association constants might be due to the increase of van der Waals interaction between alkyl side chains.

(13) The kinetic rate constants of the thermal reverse isomerization were determined at various concentrations (Figures S5, S6). The reverse isomerization was not concentration-dependent (Table S3). Therefore, the self-assembling did not influence the reverse isomerization. Dąbrowa, K.; Niedbała, P.; Jurczak, J. *Chem. Commun.* **2014**, *50*, 15748−15751.

(14) (a) Djalali, R.; Samson, J.; Matsui, H. *J. Am. Chem. Soc.* **2004**, *126*, 7935−7939. (b) Lee, E.; Kim, J. K.; Lee, M. *J. Am. Chem. Soc.* **2009**, *131*, 18242−18243.

DOI: 10.1021/acs.orglett.5b03622
Org. Lett. 2016, 18, 924−927